

On new fluorides with the Jarlite-type structure: crystal structures of $\text{Na}_2\text{Sr}_7\text{Al}_6\text{F}_{34}$, $\text{Na}_2\text{Sr}_6\text{ZnFe}_6\text{F}_{34}$ and $\text{Ba}_7\text{Ga}_6(\text{F},\text{OH})_{32}\cdot 2\text{H}_2\text{O}$

A. Hemon-Ribaud, M.P. Crosnier-Lopez, J.L. Fourquet and G. Courbion*

Laboratoire des Fluorures (U.R.A. CNRS 449), Faculté des Sciences, Route de Laval, 72017 Le Mans Cedex (France)

(Received June 9, 1993; accepted October 5, 1993)

Abstract

New compounds, $\text{Na}_2\text{Sr}_7\text{Al}_6\text{F}_{34}$, $\text{Na}_2\text{Sr}_6\text{ZnFe}_6\text{F}_{34}$ and $\text{Ba}_7\text{Ga}_6(\text{F},\text{OH})_{32}\cdot 2\text{H}_2\text{O}$, have been prepared by hydrothermal synthesis in HF solution and by the chloride flux method. The crystal structures have been resolved by X-ray diffraction. All the phases present structures of the Jarlite type in spite of having a different unit cell for the iron phase. The structures of the two first compounds are characterized by $[\text{Na}_2\text{Al}_6\text{F}_{34}]_n^{14n-}$ or $[\text{NaZnFe}_6\text{F}_{34}]_n^{13n-}$ sheets of octahedra connected by Sr or [Sr, Na] polyhedra whereas the hydrated fluoride exhibits $[\text{Ga}_3(\text{F},\text{OH})_{16}]^{7-}$ isolated octahedra trimers separated by Ba ions and water molecules. Structural correlations are made with other Jarlite type phases and with structures involving 'independent' fluoride ions.

Introduction

During the past four years, we have investigated the ternary systems $\text{NaF}-\text{SrF}_2-\text{MF}_3$ ($\text{M}=\text{Al}^{\text{III}}, \text{Fe}^{\text{III}}$) by means of solid-state syntheses, and also by hydrothermal and chloride flux growth techniques. This has allowed us to achieve the synthesis of quaternary fluorides [1–3] and a chlorofluoride [4] with new structural types. Beside these phases, three compounds with formulae related to the Jarlite type [5] – $\text{Na}_2\text{Sr}_7\text{Al}_6\text{F}_{34}$, $\text{Na}_2\text{Sr}_6\text{ZnFe}_6\text{F}_{34}$ and $\text{Ba}_7\text{Ga}_6(\text{F},\text{OH})_{32}\cdot 2\text{H}_2\text{O}$ – were found. The last compound was obtained from $\text{BaF}_2-\text{Ga}_2\text{O}_3$ binary system by means of hydrothermal synthesis in HF.

From an historical point of view, Jarlite was described for the first time by Bogvad (1933) [6], and then by Brosset [7] and Ferguson [8], and shown to have the empirical formula $\text{NaSr}_3\text{Al}_3(\text{F},\text{OH})_{16}$. The crystal structure was resolved by Hawthorne (1983) [5]; the mineral had the formula $\text{Na}(\text{Sr}_6\text{Na})\text{MgAl}_6\text{F}_{32}(\text{OH})_2$ and cationic disorder (Na, Sr) was reported for three sites.

Since the 2b and 2d special positions are occupied by Na^+ and Mg^{2+} ions respectively in the natural compound (the linked Mg and Na octahedra form a vertex-sharing $[\text{MgNaX}_{10}\equiv(\text{MX}_5)_2]$ chain), whereas in the synthetic 'deficient' $\text{Ba}_7\text{M}^{\text{II}}\text{Fe}_6\text{F}_{34}$ ($\text{M}^{\text{II}}=\text{Cu}, \text{Fe}, \text{Mn}$) compounds [9–11] the 2b special position remains empty, we decided to determine the crystal structures of the title fluorides to determine the occupancy of these sites and the possible cationic disorder.

*Author to whom correspondence should be addressed.

Experimental

All the starting materials used for experiments (NaF , SrF_2 , BaF_2 , NaCl , ZnCl_2 , Ga_2O_3) were commercial products (purity > 2 N), except FeF_3 and AlF_3 which were respectively prepared in the laboratory by heating of FeCl_3 under HF gaseous flux and by thermal decomposition of $(\text{NH}_4)_3\text{AlF}_6$.

Single crystals of $\text{Na}_2\text{Sr}_7\text{Al}_6\text{F}_{34}$ were grown by hydrothermal synthesis [12] in a sealed platinum tube from concentrated aqueous HF solutions. Typical conditions for crystal growth are listed in Table 1. After cooling, the solid was rapidly washed with ethanol and filtered. X-Ray diffraction analysis of the resulting mixture revealed that four kinds of crystals were present: NaSrAlF_6 , $\text{Na}_5\text{Al}_3\text{F}_{14}$, $\text{Na}_2\text{Sr}_7\text{Al}_6\text{F}_{34}$ and an unknown phase. Crystals of poor quality were also obtained by chloride flux growth.

Single crystals of the iron phase were synthesized using the chloride flux method in a platinum crucible under an argon atmosphere [13, 14]. The mixture ($\text{NaF} + \text{SrF}_2 + 3\text{FeF}_3 + 5.85\text{NaCl} + 3.6\text{ZnCl}_2$) was heated

TABLE 1. Conditions for crystal growth of $\text{Na}_2\text{Sr}_7\text{Al}_6\text{F}_{34}$

Volume of platinum tube	3.42 ml	Heating rate	300 °C h ⁻¹
Filling ratio	0.33	Temp. max. (T_f)	685 °C
HF (40% volume)	1 ml	Stay at T_f	24 h
$[\text{Na}_2\text{Sr}_5\text{Al}_3\text{F}_{21}]$	2 M	Cooling rate	30 °C h ⁻¹
P_{initial} (RT)	900 bar	P_{final} (T_f)	2000 bar

to 650 °C and slowly cooled (5 °C h⁻¹) to room temperature. X-Ray analysis of the crushed crystals revealed two kinds of phases: Na₃Fe₃F₁₄ (yellow) and Na₂Sr₆ZnFe₆F₃₄ (brown).

The compound Ba₇Ga₆(F,OH)₃₂·2H₂O was prepared by hydrothermal synthesis in HF solution from BaF₂ and Ga₂O₃ in a stoichiometric ratio: 1 g of this mixture was introduced with 10 cm³ of 10% HF into a Teflon bomb (Berghof), heated for 48 h at 200 °C (the pressure was close to 15 MPa) and then slowly cooled (12 °C h⁻¹). The solid phase was filtered off, washed with ethanol and air-dried. A very few colourless needles were obtained. The chemical analysis of their F content, conducted by pyrohydrolysis (F_{exp}% = 20.3 ± 1.0), revealed an F/O ratio close to 1.9, leading to the formulation Ba₇Ga₆F_{21.0}(OH)_{11.0}·2H₂O, and TGA experiments showed a 3.7% weight loss starting at 120 °C (Δ*m*_{theo} = 1.8%).

X-Ray data collection

X-Ray intensity data collection was performed on an AED2-SIEMENS STOE four-circle diffractometer (Mo Kα) for the three compounds. The lattice parameters were refined from the positions of 32 centred reflections for Na₂Sr₇Al₆F₃₄ (40 reflections for Na₂Sr₆ZnFe₆F₃₄ and 32 reflections for Ba₇Ga₆(F,OH)₃₂·2H₂O) in the vicinity of 30° (2θ) by the double scan technique. The conditions for the diffraction experiments are summarized in Table 2. The observed unit cells are in agreement with the Jarlite-type except for Na₂Sr₆ZnFe₆F₃₄ where a doubling of the *c* parameter is present.

Structure determination

All the calculations were performed using the SHELX-76 program [16]. Atomic scattering factors and anomalous dispersion corrections were taken from *International Tables for X-ray Crystallography* [17].

Na₂Sr₇Al₆F₃₄ and Ba₇Ga₆(F,OH)₃₂·2H₂O

The limiting condition for the observed reflections – *hkl* with *h + k = 2n* – led to the possible space groups C2/*m*, C2 and *Cm*. In the centric space group, the structure was solved using the interpretation of a Patterson map in the range 4 < 2θ < 50° (option PATT of SHELXS-86 [18]) which provided the positions of the cations. Difference Fourier synthesis allowed completion of the structures and revealed the anionic sites. The final refinement with anisotropic thermal motion dropped to *R* = 0.026 and *R*_w = 0.029 for Na₂Sr₇Al₆F₃₄ and *R* = 0.029 and *R*_w = 0.031 for Ba₇Ga₆(F,OH)₃₂·2H₂O. Tables 3 and 4 list the atomic coordinates and thermal motion parameters, whereas Tables 5 and 6 list the main interatomic distances and angles. Attempts

to refine this structure in the noncentric C2 and *Cm* space groups did not give improvement of the *R* factor.

It is noteworthy that, in the case of the barium compound, two sites (2b and 2d) of the Jarlite-type are empty. Moreover, as in all such compounds [20, 21], it was impossible to distinguish between O²⁻ and F⁻ from X-ray diffraction data. For this reason, bond valence calculations [22] were undertaken in order to clear up this question and these showed unambiguously that the water molecules are on site 10 (see Table 7) (quoted as OW in Table 4). The hydrogen of the H₂O molecules and the hydroxyl groups were impossible to locate even when limiting the data collection to lower 2θ values. Hence, under these conditions, we can only suggest that OH⁻ and F⁻ ions are statistically located on the nine other anionic sites, quoted X(*i*).

Na₂Sr₆ZnFe₆F₃₄

Examination of the conditions limiting the possible reflections – *hkl*, *h + k = 2n* and *h0l*, *l = 2n* – led to the possible space group C2/*c* (and the non-centric groups C2, *Cc*). However, the *hkl* observed reflections with *l ≠ 2n* were systematically weak. The most intense with odd *l* had an intensity which represented only 4% of the maximal reflection. Moreover, in the parity groups of observed reflections, 75% of the reflections with *l* even were retained (*I*/*σ*(*I*) > 3) whereas only 35% with *l* odd. Therefore, as a first step, a minimal subcell was considered with the parameters *a*, *b*, *c*/2 (*a*, *b*, *c* being the parameters listed in Table 2); in this subcell, the observed extinctions were in agreement with the Jarlite space group C2/*m*. Starting from the Na₂Sr₇Al₆F₃₄ model, successive refinements led to a reliability factor *R* = 0.115 with isotropic thermal motions (2261 reflections, 59 parameters). This result was obtained after interatomic distance and thermal motion analysis. The 2d site was occupied by a zinc ion rather than a sodium cation and the strontium sites, 4i and 8j, were occupied in a statistical manner by Na and Sr ions. Very high isotropic thermal motions for the fluorine atoms F(5) and F(7) (*B*_{eq} ≈ 7 Å²) were observed indicating that they were mainly responsible for the superstructure.

In a second step, the model was then extended to the supercell using the space group C2/*c*. With a correct choice of the origin, the reliability factor dropped to *R* = 0.09 with isotropic thermal motion and to *R* = 0.067 (*R*_w = 0.067) when applying anisotropic thermal motion. Attempts to refine the data with absorption corrections or in non-centric space groups did not improve the *R* factor. Despite the poor reliability factor, but taking into account the absence of any anomaly in the crystal chemistry, the final results obtained are presented in Table 8. Table 9 gives the main interatomic distances.

TABLE 2. Crystal data and conditions of data collection and refinement for Na₂Sr₇Al₆F₃₄, Na₂Sr₆ZnFe₆F₃₄ and Ba₇Ga₆(F,OH)₃₂·2H₂O

	Na ₂ Sr ₇ Al ₆ F ₃₄	Na ₂ Sr ₆ ZnFe ₆ F ₃₄	Ba ₇ Ga ₆ (F,OH) ₃₂ ·2H ₂ O
Symmetry	Monoclinic	Monoclinic	Monoclinic
Space group	C2/m (No. 12)	C2/c (No. 15)	C2/m (No. 12)
Cell parameters	$a = 16.072(3) \text{ \AA}$ $b = 10.822(1) \text{ \AA}$ $c = 7.258(1) \text{ \AA}$ $\beta = 101.23(1)^\circ$ $V = 1238.2 \text{ \AA}^3$ $Z = 2$	$a = 16.167(3) \text{ \AA}$ $b = 11.013(1) \text{ \AA}$ $c = 15.090(2) \text{ \AA}$ $\beta = 101.72(1)^\circ$ $V = 2630.9 \text{ \AA}^3$ $Z = 4$	$a = 16.908(2) \text{ \AA}$ $b = 11.406(1) \text{ \AA}$ $c = 7.542(1) \text{ \AA}$ $\beta = 101.28(1)^\circ$ $V = 1426.4 \text{ \AA}^3$ $Z = 2$
Density	$d_{\text{calc}} = 3.94 \text{ g cm}^{-3}$	$d_{\text{calc}} = 4.09 \text{ g cm}^{-3}$	$d_{\text{calc}} = 4.66 \text{ g cm}^{-3}$
Crystal volume (10 ⁻³ mm ³)	4.9	1.8	0.2
Radiation		Mo K α (graphite monochromatized)	
Scanning mode		$\omega/2\theta$, time per step: 1–4 s	
Aperture (mm)		3.5 × 3.5	
Profile fitting data analysis [15]	Isotropic linewidth, $w = (0.76 + 0.37 \tan \theta)^\circ$	Isotropic linewidth, $w = (0.95 + 0.05 \tan \theta)^\circ$	None
Range registered $\theta_{\text{min}}, \theta_{\text{max}}(^\circ)$	2.00, 45.00	2.00, 35.00	2.00, 32.50
h, k, l_{max}	31, 21, 14	26, 17, 24	25, 17, 11
Absorption coefficient	$\mu = 150.13 \text{ cm}^{-1}$	$\mu = 161.24 \text{ cm}^{-1}$	$\mu = 151.83 \text{ cm}^{-1}$
Absorption correction	Gaussian method	None	Gaussian method
Transmission factors	max: 0.20 min: 0.08	–	max: 0.65 min: 0.48
Reflections measured:			
Total	6228 (1.5 sets)	6226 (1 set)	2834 (1 set)
Independent (R_{av})	4848 ($R = 0.017$)	4964	2470
Used in refinement	3856 ($I_o > 3\sigma(I_o)$)	3300 ($I_o > 3\sigma(I_o)$)	1716 ($I_o > 3\sigma(I_o)$)
Number of refined parameters	125	228	116
Weighting scheme	$W = 1.5/(\sigma^2(F) + 2 \times 10^{-4}F^2)$	None	$W = 1.0/(\sigma^2(F) + 9 \times 10^{-4}F^2)$
Secondary extinction	$\epsilon = 1.02(5) \times 10^{-7}$	None	None
Maximum height in final Fourier difference map	0.1 e ⁻ Å ⁻³ (close to Sr(3))	0.4 e ⁻ Å ⁻³ (close to X(2))	1.1 e ⁻ Å ⁻³ (close to 2d site)

TABLE 3. Atomic coordinates, anisotropic temperature factors $U_{ij} \times 10^4$ and B_{eq} (Å²) for Na₂Sr₇Al₆F₃₄

Atom	Site	x	y	z	U_{11}	U_{22}	U_{33}	U_{23}	U_{13}	U_{12}	B_{eq}
Sr(1)	2a	0	0	0	62(1)	105(1)	122(1)	0	7(1)	0	0.77
Sr(2)	4i	0.26095(1)	0	0.12281(3)	97(1)	97(1)	128(1)	0	27(1)	0	0.84
Sr(3)	8j	0.14543(1)	0.30113(1)	0.30265(2)	77(1)	116(1)	90(1)	-3(0)	12(0)	16(0)	0.75
Al(1)	4i	0.16876(4)	0	0.5441(1)	82(3)	65(2)	60(3)	0	18(2)	0	0.54
Al(2)	8j	0.11009(3)	0.2428(1)	0.7991(1)	67(2)	74(2)	61(2)	1(1)	20(1)	4(1)	0.52
Na(1)	2d	0	1/2	1/2	78(5)	104(5)	88(6)	0	33(4)	0	0.69
Na(2)	2b	0	1/2	0	133(7)	260(9)	119(7)	0	-17(5)	0	1.39
F(1)	8j	0.3836(1)	0.1306(1)	0.0354(2)	149(4)	102(4)	110(4)	-25(3)	35(3)	-1(3)	0.94
F(2)	8j	0.4052(1)	0.1487(1)	0.3899(2)	217(5)	223(5)	128(5)	82(4)	71(4)	79(4)	1.45
F(3)	8j	0.2783(1)	0.2409(1)	0.1883(2)	83(3)	154(4)	132(4)	-1(3)	35(3)	-8(3)	0.96
F(4)	8j	0.1305(1)	0.1323(1)	0.9943(2)	109(4)	117(4)	152(5)	57(3)	23(3)	0(3)	1.00
F(5)	8j	0.2312(1)	0.1165(1)	0.4570(2)	143(4)	161(5)	174(5)	61(4)	16(4)	-55(4)	1.27
F(6)	8j	0.0002(1)	0.2210(1)	0.7955(2)	77(3)	210(5)	171(5)	-8(4)	26(3)	13(3)	1.20
F(7)	8j	0.1066(1)	0.1171(1)	0.6292(2)	124(4)	203(5)	251(6)	-146(5)	-11(4)	47(4)	1.57
F(8)	4i	0.2462(1)	0	0.7622(2)	101(5)	168(6)	101(6)	0	-11(5)	0	1.00
F(9)	4i	0.1020(1)	0	0.3167(3)	189(7)	262(9)	87(7)	0	-20(6)	0	1.46
F(10)	4i	0.4235(1)	0	0.7188(2)	129(6)	103(5)	104(6)	0	23(5)	0	0.88

TABLE 4. Atomic coordinates, anisotropic temperature factors $U_{ij} \times 10^4$ and B_{eq} (\AA^2) for $\text{Ba}_7\text{Ga}_6(\text{F},\text{OH})_{32} \cdot 2\text{H}_2\text{O}$ ($\text{X} = \text{F}, \text{OH}$)

Atom	Site	<i>x</i>	<i>y</i>	<i>z</i>	U_{11}	U_{22}	U_{33}	U_{23}	U_{13}	U_{12}	B_{eq}
Ba(1)	2a	0	0	0	101(3)	81(3)	131(3)	0	14(3)	0	0.84
Ba(2)	4i	0.2660(1)	0	0.1324(3)	138(2)	102(2)	133(2)	0	43(2)	0	1.02
Ba(3)	8j	0.1408(1)	0.2946(1)	0.3037(2)	147(2)	190(2)	142(2)	-17(2)	27(1)	-15(1)	1.29
Ga(1)	4i	0.1741(1)	0	0.5469(1)	130(4)	77(4)	81(4)	0	23(3)	0	0.78
Ga(2)	8j	0.1114(1)	0.2414(1)	0.7992(1)	127(3)	81(3)	113(3)	2(2)	49(2)	-6(2)	0.89
X(1)	8j	0.3852(3)	0.1345(4)	0.0347(6)	227(21)	96(17)	148(18)	-47(15)	85(16)	-13(15)	1.46
X(2)	8j	0.4056(3)	0.1458(5)	0.3868(6)	384(27)	292(27)	195(22)	119(20)	116(20)	74(21)	2.41
X(3)	8j	0.2781(2)	0.2424(4)	0.1912(6)	167(18)	198(21)	240(22)	-24(18)	117(17)	-31(16)	1.71
X(4)	8j	0.1331(2)	0.1331(4)	0.9963(6)	163(18)	121(18)	218(20)	67(16)	26(16)	-28(15)	1.35
X(5)	8j	0.2362(3)	0.1151(4)	0.4569(6)	273(22)	164(21)	198(20)	19(17)	44(17)	-78(17)	1.72
X(6)	8j	0.0029(2)	0.2084(4)	0.7939(6)	150(17)	202(21)	234(21)	14(18)	49(16)	1(16)	1.59
X(7)	8j	0.1098(3)	0.1187(5)	0.6195(7)	250(22)	274(27)	399(30)	-181(24)	90(21)	54(20)	2.52
X(8)	4i	0.2533(4)	0	0.7598(8)	191(28)	216(31)	106(26)	0	1(22)	0	1.35
X(9)	4i	0.1098(4)	0	0.3134(9)	292(34)	357(41)	125(29)	0	-66(26)	0	1.97
OW	4i	0.4616(6)	0	0.7350(15)	339(49)	209(44)	579(69)	0	108(47)	0	3.08

TABLE 5. Main interatomic distances (\AA) in $\text{Na}_2\text{Sr}_7\text{Al}_6\text{F}_{34}$

<i>Sr(1) polyhedron [CN=10]</i>	<i>Sr(2) polyhedron [CN=9]</i>	<i>Sr(3) polyhedron [CN=9]</i>
Sr(1)–F(4) = 4 × 2.546(1)	Sr(2)–F(4) = 2 × 2.560(1)	Sr(3)–F(10) = 2.412(1)
Sr(1)–F(9) = 2 × 2.550(2)	Sr(2)–F(8) = 2.582(2)	Sr(3)–F(6) = 2.467(1)
Sr(1)–F(6) = 4 × 2.815(1)	Sr(2)–F(1) = 2 × 2.603(1)	Sr(3)–F(1) = 2.518(1)
⟨Sr(1)–F⟩ = 2.65	Sr(2)–F(3) = 2 × 2.655(1)	Sr(3)–F(3) = 2.522(1)
$d_{\text{Shannon}} [19] = 2.661$	Sr(2)–F(5) = 2 × 2.855(1)	Sr(3)–F(5) = 2.534(1)
	⟨Sr(2)–F⟩ = 2.66	Sr(3)–F(5) = 2.558(1)
	$d_{\text{Shannon}} = 2.618$	Sr(3)–F(2) = 2.578(1)
		Sr(3)–F(4) = 2.863(1)
		Sr(3)–F(8) = 2.865(1)
		⟨Sr(3)–F⟩ = 2.59
	<i>Al(1) octahedron</i>	<i>Al(2) octahedron</i>
	Al(1)–F(9) = 1.785(1)	Al(2)–F(6) = 1.777(1)
	Al(1)–F(7) = 2 × 1.796(1)	Al(2)–F(2) = 1.786(1)
	Al(1)–F(5) = 2 × 1.800(1)	Al(2)–F(3) = 1.788(1)
	Al(1)–F(8) = 1.813(1)	Al(2)–F(1) = 1.811(1)
	⟨Al(1)–F⟩ = 1.80	Al(2)–F(7) = 1.830(1)
	$d_{\text{Shannon}} = 1.815$	Al(2)–F(4) = 1.834(1)
		⟨Al(2)–F⟩ = 1.80
	<i>Na(1) octahedron</i>	<i>Na(2) octahedron</i>
	Na(1)–F(10) = 2 × 2.189(1)	Na(2)–F(10) = 2 × 2.168(1)
	Na(1)–F(2) = 4 × 2.253(1)	Na(2)–F(1) = 4 × 2.398(1)
	⟨Na(1)–F⟩ = 2.23	⟨Na(2)–F⟩ = 2.32
	$d_{\text{Shannon}} = 2.33$	

A table specifying the calculated and observed structure factors for the compounds can be obtained on request from the authors.

Structure description and discussion

$\text{Na}_2\text{Sr}_7\text{Al}_6\text{F}_{34}$ and $\text{Na}_2\text{Sr}_6\text{ZnFe}_6\text{F}_{34}$: no 'deficient' Jarlite

The structures of these two new fluorides are isotopic with natural Jarlite. All the cations, except Sr^{2+} , are octahedrally surrounded by fluorine atoms. The mean Al–F and Fe–F distances (1.80 Å and 1.92 Å, re-

spectively) are very close to the sum of the ionic radii [19] as well as to the mean $\text{M}^{\text{III}}\text{–F}$ distances encountered in aluminium [23] and iron [24] fluoride compounds for six-fold coordination. However, the $\text{Na}_2\text{Sr}_6\text{ZnFe}_6\text{F}_{34}$ phase has a double volume because its *c* parameter is twice as large as in $\text{Na}_2\text{Sr}_7\text{Al}_6\text{F}_{34}$; (100) projections (Fig. 1) of both phases show these features. It can be seen that the different cell volumes are mainly dependent on the tilting modes of the octahedra. Figure 2(a) shows a perspective view of the $\text{Na}_2\text{Sr}_7\text{Al}_6\text{F}_{34}$ structure: stacking of aluminium and sodium octahedra is obvious. The octahedra build up (*b*, *c*) planes of formulation $[\text{Na}_2\text{Al}_6\text{F}_{34}]_n^{14n-}$ containing $[\text{Al}_3\text{F}_{16}]_7^{7-}$ trimers and

TABLE 6. Main interatomic distances (Å) in $\text{Ba}_7\text{Ga}_6(\text{F},\text{OH})_{32}\cdot 2\text{H}_2\text{O}$ (X = F, OH)

<i>Ba(1) polyhedron [CN=10]</i>	<i>Ba(2) polyhedron [CN=9]</i>	<i>Ba(3) polyhedron [CN=9]</i>
Ba(1)–X(9) = 2 × 2.708(6)	Ba(2)–X(4) = 2 × 2.744(4)	Ba(3)–X(6) = 2.595(3)
Ba(1)–X(4) = 4 × 2.724(4)	Ba(2)–X(1) = 2 × 2.750(5)	Ba(3)–X(1) = 2.635(4)
Ba(1)–X(6) = 4 × 2.852(5)	Ba(2)–X(8) = 2.780(6)	Ba(3)–X(5) = 2.683(4)
⟨Ba(1)–X⟩ = 2.77	Ba(2)–X(3) = 2 × 2.808(4)	Ba(3)–X(3) = 2.693(4)
$d_{\text{Shannon}}(\text{Ba}–\text{F}) = 2.805$	Ba(2)–X(5) = 2 × 2.911(5)	Ba(3)–X(2) = 2.695(5)
	⟨Ba(2)–X⟩ = 2.80	Ba(3)–X(5) = 2.726(4)
	$d_{\text{Shannon}}(\text{Ba}–\text{F}) = 2.755$	Ba(3)–O = 2.900(6)
		Ba(3)–X(4) = 2.949(5)
		Ba(3)–X(8) = 3.049(4)
		⟨Ba(3)–X⟩ = 2.77
	<i>Ga(1) octahedron</i>	<i>Ga(2) octahedron</i>
	Ga(1)–X(8) = 1.881(6)	Ga(2)–X(3) = 1.867(3)
	Ga(1)–X(9) = 1.882(6)	Ga(2)–X(6) = 1.868(3)
	Ga(1)–X(7) = 2 × 1.887(6)	Ga(2)–X(2) = 1.887(5)
	Ga(1)–X(5) = 1.892(5)	Ga(2)–X(1) = 1.887(5)
	⟨Ga(1)–X⟩ = 1.89	Ga(2)–X(4) = 1.916(4)
	$d_{\text{Shannon}}(\text{Ga}–\text{F}) = 1.905$	Ga(2)–X(7) = 1.949(6)
		⟨Ga(2)–X⟩ = 1.90

TABLE 7. Calculated valence S for the anionic sites^a in $\text{Ba}_7\text{Ga}_6(\text{F},\text{OH})_{32}\cdot 2\text{H}_2\text{O}$

	Ga(1)	Ga(2)	Ba(1)	Ba(2)	Ba(3)	ΣS_i
Site 1 O		0.65		0.29	0.39	1.33
F		0.49		0.22	0.30	1.01
Site 2 O		0.65			0.33	0.98
F		0.49			0.26	0.75
Site 3 O		0.69		0.25	0.34	1.28
F		0.51		0.19	0.26	0.96
Site 4 O		0.61	0.31	0.29	0.17	1.38
F		0.45	0.24	0.22	0.13	1.04
Site 5 O	0.65			0.19	0.35–0.31	1.50
F	0.48			0.14	0.26–0.24	1.12
Site 6 O		0.69	0.22		0.44	1.35
F		0.51	0.17		0.34	1.02
Site 7 O	0.65	0.55				1.20
F	0.49	0.41				0.90
Site 8 O	0.66		0.13–0.13	0.27		1.19
F	0.49		0.10–0.10	0.20		0.89
Site 9 O	0.66		0.32			0.98
F	0.49		0.25			0.74
Site 10 O					0.19–0.19	0.38
F					0.15–0.15	0.30

^aFor sites i , $S_i = \sum_j \exp[(R_{ij} - d_{ij})/b]$ with $b = 0.37$ and R_{ij} for oxygen and fluorine respectively 2.29 and 2.19 for Ba^{2+} , and 1.73 and 1.62 for Ga^{3+} [22].

$[\text{Na}_2\text{F}_{10}]_n^{8n-}$ corrugated chains along the c -axis. In the $[\text{Al}_3\text{F}_{16}]_n^{7-}$ trimers, the Al(1) octahedron is *cis*-connected to two Al(2) octahedra by corner-sharing [Al(1)–F(7)–Al(2) = 144.1(1)°]. The $[\text{Na}_2\text{F}_{10}]_n^{8n-}$ chains arise from Na(1) and Na(2) octahedra connecting at opposite corners [Fig. 1(a)]. The same features are observed in the $\text{Na}_2\text{Sr}_6\text{ZnFe}_6\text{F}_{34}$ compound, but one sodium ion is replaced by a zinc cation: $[\text{NaZn}$

$\text{F}_{34}]_n^{13n-}$ sheets parallel to (b , c) planes built up from $[\text{Fe}_3\text{F}_{16}]_n^{7-}$ trimers of octahedra [Fe(1)–F(7a)–Fe(2a) = 137.2(3)° and Fe(1)–F(7b)–Fe(2b) = 137.7(4)°] and $[\text{NaZnF}_{10}]_n^{7n-}$ chains running along the c -axis. The main difference between these structures concerns the strontium polyhedra. Firstly, in $\text{Na}_2\text{Sr}_7\text{Al}_6\text{F}_{34}$, the strontium ions are nine- and ten-fold coordinated whereas in $\text{Na}_2\text{Sr}_6\text{ZnFe}_6\text{F}_{34}$ they are eight- and ten-fold coordinated. Secondly, a cationic disorder (Na, Sr) is observed for three sites in $\text{Na}_2\text{Sr}_6\text{ZnFe}_6\text{F}_{34}$ (indicated as X in Table 8), whereas in $\text{Na}_2\text{Sr}_7\text{Al}_6\text{F}_{34}$ each site – 2a, 4i, 8j – is fully occupied by strontium ions. A similar cationic disorder was found earlier by Hawthorne in the mineral. The different occupation ratio (Na, Sr) for the X sites are compared in Table 10. It is observed when one Sr^{2+} is replaced by a smaller M^{2+} ion (Mg^{2+} or Zn^{2+}), octahedral coordination is preferentially adopted. Hence one sodium ion becomes statistically distributed with the strontium cations on the X sites. In the case of $\text{Na}_2\text{Sr}_6\text{ZnFe}_6\text{F}_{34}$, one site (4a in Table 8) remains fully occupied by a strontium atom.

Another feature of these phases pertains to the existence of an ‘independent’ fluorine F(10) besides those bonded to the trivalent cations; such ions have been encountered previously in other fluorides [25], e.g. $\text{Na}_2\text{Ca}_3\text{Al}_2\text{F}_{14}$ [26], NaCdAlF_6 [27], $\text{NaSr}_2\text{CrF}_8$ [28] and the two forms of Ba_3AlF_9 [29, 30]. However, in $\text{Na}_2\text{Sr}_7\text{Al}_6\text{F}_{34}$, this independent fluoride is not surrounded tetrahedrally by cations but forms infinite zigzag files $[\text{NaF}]_n$ with sodium ions along the [001] direction ($[\text{NaZnF}_2]_n$ files in $\text{Na}_2\text{Sr}_6\text{ZnFe}_6\text{F}_{34}$).

TABLE 8. Atomic coordinates, anisotropic temperature factors $U_{ij} \times 10^4$ and B_{eq} (\AA^2) for $\text{Na}_2\text{Sr}_6\text{ZnFe}_6\text{F}_{34}$

Atom ^a	Site	x	y	z	U_{11}	U_{22}	U_{33}	U_{23}	U_{13}	U_{12}	B_{eq}
Sr(1)	4a	0	0	0	103(6)	127(6)	184(7)	-9(7)	-13(5)	12(7)	1.10
X(2) ^b	8f	0.2578(1)	-0.0050(1)	0.0503(1)	159(7)	94(6)	228(7)	23(6)	35(5)	3(6)	1.23
X(3a) ^b	8f	0.1516(1)	0.3120(1)	0.1517(1)	131(8)	140(6)	166(8)	26(5)	12(6)	6(5)	1.14
X(3b) ^b	8f	0.1500(1)	0.2969(1)	0.6505(1)	139(8)	153(7)	147(8)	12(5)	14(6)	1(5)	1.14
Fe(1)	8f	0.1661(1)	0.0047(2)	0.2661(1)	173(7)	51(6)	87(6)	-3(6)	37(5)	9(7)	0.78
Fe(2a)	8f	0.1042(1)	0.2433(2)	0.4037(1)	114(8)	39(6)	97(8)	1(5)	16(7)	4(5)	0.64
Fe(2b)	8f	0.1099(1)	0.2509(2)	0.8966(1)	121(8)	46(6)	89(8)	-1(6)	9(7)	8(6)	0.66
Zn(1)	4e	0	0.4935(3)	1/4	237(10)	171(10)	211(10)	0	45(8)	0	1.58
Na(1)	4b	0	1/2	0	202(35)	249(38)	171(33)	-20(40)	-4(27)	-1(41)	1.64
F(1a)	8f	0.3843(6)	0.1283(7)	0.0110(6)	233(47)	68(29)	147(39)	-56(27)	51(37)	-7(28)	1.12
F(1b)	8f	0.3841(6)	0.01227(7)	0.5123(6)	226(46)	48(28)	158(39)	-20(27)	19(36)	-13(28)	1.12
F(2a)	8f	0.4167(6)	0.1474(9)	0.7001(7)	211(44)	235(42)	232(46)	162(36)	-36(36)	26(35)	1.82
F(2b)	8f	0.4089(8)	0.1185(9)	0.1937(7)	530(74)	206(43)	246(51)	172(39)	152(52)	99(45)	2.42
F(3a)	8f	0.2789(6)	0.2432(9)	0.5912(7)	167(41)	260(42)	171(40)	-3(36)	42(34)	-15(35)	1.53
F(3b)	8f	0.2719(6)	0.2217(8)	0.0947(7)	219(47)	163(37)	234(46)	-48(33)	42(38)	-54(32)	1.58
F(4a)	8f	0.1276(6)	0.1360(7)	0.5093(6)	185(39)	59(28)	219(42)	71(27)	5(33)	8(27)	1.21
F(4b)	8f	0.1290(6)	0.1174(7)	0.9799(7)	224(44)	100(32)	270(46)	117(31)	43(37)	3(30)	1.52
F(5a)	8f	0.2407(7)	0.0955(9)	0.7127(7)	261(49)	259(46)	348(54)	139(41)	89(42)	-94(38)	2.19
F(5b)	8f	0.2234(6)	0.1485(8)	0.2418(7)	281(49)	151(37)	285(48)	66(34)	69(40)	-61(33)	1.81
F(6a)	8f	0.0112(6)	0.2285(8)	0.0935(7)	142(40)	175(37)	307(50)	14(34)	46(37)	-1(31)	1.59
F(6b)	8f	0.0056(6)	0.2252(9)	0.6098(8)	146(43)	262(45)	350(56)	44(41)	22(40)	39(35)	1.97
F(7a)	8f	0.0945(6)	0.0972(8)	0.3284(7)	186(40)	186(38)	312(48)	-196(36)	52(36)	-18(31)	1.74
F(7b)	8f	0.1140(6)	0.1470(7)	0.7906(6)	282(47)	119(33)	234(43)	-82(31)	11(37)	71(32)	1.66
F(8)	8f	0.2527(5)	-0.0067(8)	0.3769(5)	200(34)	149(33)	151(31)	7(32)	-18(26)	27(33)	1.33
F(9)	8f	0.0972(7)	0.0151(11)	0.1504(6)	467(60)	306(51)	175(38)	30(43)	-45(37)	76(50)	2.54
F(10)	8f	0.4380(5)	0.0002(8)	0.3526(5)	207(34)	141(30)	121(28)	17(33)	-25(24)	-53(36)	1.26

^aSame atom labelling as for $\text{Na}_2\text{Sr}_7\text{Al}_6\text{F}_{34}$, the site degeneration is marked by letters a and b; the b position is obtained from the a position by a translation close to 0 0 1/2.

^bRefined occupation ratio:

	Site	Sr	Na
X(2)	8f	0.78(1)	0.22(1)
X(3a)	8f	0.88(1)	0.12(1)
X(3b)	8f	0.86(1)	0.14(1)
Total	24	20.16 \approx 20	3.84 \approx 4

$\text{Ba}_7\text{Ga}_6(\text{F}, \text{OH})_{32} \cdot 2\text{H}_2\text{O}$: a 'very deficient' Jarlite and structural correlations

The structure of $\text{Ba}_7\text{Ga}_6(\text{F}, \text{OH})_{32} \cdot 2\text{H}_2\text{O}$ remains basically the same as that previously described, but in this hydrated fluoride the 2b and 2d special positions are empty and a 4i site is occupied by an oxygen ion of a water molecule instead of a fluoride ion [F(10) in $\text{Na}_2\text{Sr}_7\text{Al}_6\text{F}_{34}$]. Hence the $[\text{Na}_2\text{Al}_6\text{F}_{34}]_n^{14n-}$ planes [Fig. 2(a)] are replaced by isolated octahedra trimers $[\text{Ga}_3(\text{F}, \text{OH})_{16}]_7^-$ as shown in Fig. 2(b) $[\text{Ga}(1)-\text{X}(7)-\text{Ga}(2)=144.2(2)^\circ]$. Cohesion of the structure is brought about by barium polyhedra which ensure the connection between the isolated trimers, and also probably via $\text{O}-\text{H} \cdots \text{F}$ hydrogen bonds. The geometry of such bonds has been summarized by Simonov and Bukvetsky [31] from an analysis of the structures of metal fluoride crystal hydrates. They have shown that the $\text{O} \cdots \text{F}$ distances between the atoms

involved in hydrogen bonding range from 2.56 to 2.86 \AA , with an average value equal to 2.68 \AA . Hence, in $\text{Ba}_7\text{Ga}_6(\text{F}, \text{OH})_{32} \cdot 2\text{H}_2\text{O}$, the water molecules do not take part in such bonding (the shortest $\text{OW}-\text{F}$ distance is equal to 3.08 \AA), but the nine other anions can give this kind of hydrogen bond.

Structural correlations can be made with the Jarlite and with the 'deficient' Jarlite $\text{Ba}_7\text{M}^{\text{II}}\text{Fe}_6\text{F}_{34}$ ($\text{M}^{\text{II}} = \text{Mn}, \text{Fe}, \text{Cu}$) [9-11]. These compounds can be differentiated by cationic occupation in the 2b and 2d sites as reported in Table 11. Indeed, according to the site vacancy level, helicoidal double chains $[\square\text{MFe}_6\text{F}_{34}]_n$ can be observed running along the *b*-axis with a 2b site empty for $\text{Ba}_7\text{M}^{\text{II}}\text{Fe}_6\text{F}_{34}$ compounds or isolated octahedral trimers $[\square_2\text{Ga}_6(\text{F}, \text{OH})_{32}] \equiv [\text{Ga}_3(\text{F}, \text{OH})_{16}]_2$ when the 2b and 2d sites remain empty in $\text{Ba}_7\text{Ga}_6(\text{F}, \text{OH})_{32} \cdot 2\text{H}_2\text{O}$ rather than $[\text{Na}_2\text{Al}_6\text{F}_{34}]_n^{14n-}$ planes as in $\text{Na}_2\text{Sr}_7\text{Al}_6\text{F}_{34}$ (Fig. 3). This feature is responsible for the 1D ferrimagnetic

TABLE 9. Main interatomic distances (Å) in Na₂Sr₆ZnFe₆F₃₄

<i>Sr(1) polyhedron [CN=10]</i>		<i>X(2) polyhedron [CN=8]</i>			
Sr(1)–F(9) = 2 × 2.490(8)		X(2)–F(4a) = 2.523(8)			
Sr(1)–F(4b) = 2 × 2.525(9)		X(2)–F(4b) = 2.526(8)			
Sr(1)–F(4a) = 2 × 2.530(8)		X(2)–F(1b) = 2.580(9)			
Sr(1)–F(6a) = 2 × 2.873(9)		X(2)–F(3b) = 2.582(8)			
Sr(1)–F(6b) = 2 × 2.973(10)		X(2)–F(8) = 2.603(8)			
⟨Sr(1)–F⟩ = 2.68		X(2)–F(1a) = 2.680(9)			
<i>d</i> _{Shannon} = 2.66		X(2)–F(3a) = 2.701(9)			
		X(2)–F(5a) = 2.711(11)			
		⟨X(2)–F⟩ = 2.61			
<i>X(3a) polyhedron [CN=8]</i>		<i>X(3b) polyhedron [CN=10]</i>			
X(3a)–F(5b) = 2.408(9)		X(3b)–F(5b) = 2.417(9)			
X(3a)–F(6a) = 2.442(9)		X(3b)–F(6b) = 2.424(10)			
X(3a)–F(3b) = 2.488(11)		X(3b)–F(3a) = 2.499(10)			
X(3a)–F(1a) = 2.493(8)		X(3b)–F(1b) = 2.563(8)			
X(3a)–F(10) = 2.522(8)		X(3b)–F(10) = 2.644(8)			
X(3a)–F(5a) = 2.610(9)		X(3b)–F(5a) = 2.718(9)			
X(3a)–F(8) = 2.615(8)		X(3b)–F(4a) = 2.739(8)			
X(3a)–F(2a) = 2.724(11)		X(3b)–F(7b) = 2.834(9)			
⟨X(3a)–F⟩ = 2.54		X(3b)–F(2b) = 2.866(12)			
		X(3b)–F(8) = 2.873(8)			
		⟨X(3b)–F⟩ = 2.66			
<i>Fe(1) octahedron</i>		<i>Fe(2a) octahedron</i>		<i>Fe(2b) octahedron</i>	
Fe(1)–F(9) = 1.874(8)		Fe(2a)–F(6a) = 1.880(10)		Fe(2b)–F(6b) = 1.870(10)	
Fe(1)–F(5b) = 1.908(9)		Fe(2a)–F(3a) = 1.883(10)		Fe(2b)–F(3b) = 1.913(10)	
Fe(1)–F(7a) = 1.924(10)		Fe(2a)–F(1b) = 1.929(8)		Fe(2b)–F(1a) = 1.915(8)	
Fe(1)–F(5a) = 1.928(11)		Fe(2a)–F(2a) = 1.950(9)		Fe(2b)–F(4b) = 1.918(8)	
Fe(1)–F(7b) = 1.939(9)		Fe(2a)–F(7a) = 1.957(9)		Fe(2b)–F(2b) = 1.962(10)	
Fe(1)–F(8) = 1.955(7)		Fe(2a)–F(4a) = 1.958(8)		Fe(2b)–F(7b) = 1.979(9)	
⟨Fe(1)–F⟩ = 1.92		⟨Fe(2a)–F⟩ = 1.93		⟨Fe(2b)–F⟩ = 1.93	
<i>d</i> _{Shannon} = 1.93					
<i>Zn(1) octahedron</i>		<i>Na(1) octahedron</i>			
Zn(1)–F(10) = 2 × 2.010(8)		Na(1)–F(10) = 2 × 2.246(6)			
Zn(1)–F(2b) = 2 × 2.068(11)		Na(1)–F(1b) = 4 × 2.348(9)			
Zn(1)–F(2a) = 2 × 2.092(9)		⟨Na(1)–F⟩ = 2.32			
⟨Zn(1)–F⟩ = 2.06		<i>d</i> _{Shannon} = 2.33			
<i>d</i> _{Shannon} = 2.04					

TABLE 10. Occupation ratio (Sr, Na) in Jarlite and Na₂Sr₆ZnFe₆F₃₄

	X(1)		X(2)		X(3)			
	Sr	Na	Sr	Na	Sr	Na		
Na ₂ Sr ₆ ZnFe ₆ F ₃₄	1	0	0.78	0.22	X(3a) 0.88	X(3b) 0.86	X(3a) 0.12	X(3b) 0.14
Na ₂ Sr ₆ MgAl ₆ F ₃₂ (OH) ₂ (mineral)	0.91	0.09	0.81	0.19	0.87		0.13	

TABLE 11. Cationic repartition in the 2b and 2d sites in the C₂/m space group

	Na(Sr ₆ Na)MgAl ₆ F ₃₂ (OH) ₂	Na(Sr ₆ Na)ZnFe ₆ F ₃₄ ^a	Na ₂ Sr ₇ Al ₆ F ₃₄	Ba ₇ CuFe ₆ F ₃₄	Ba ₇ Ga ₆ (F,OH) ₃₂ ·2H ₂ O
Site 2b	Na ⁺	Na ⁺	Na ⁺	–	–
Site 2d	Mg ²⁺	Zn ²⁺	Na ⁺	Cu ²⁺	–

^aDescription given in the C₂/m space group instead of C₂/c.

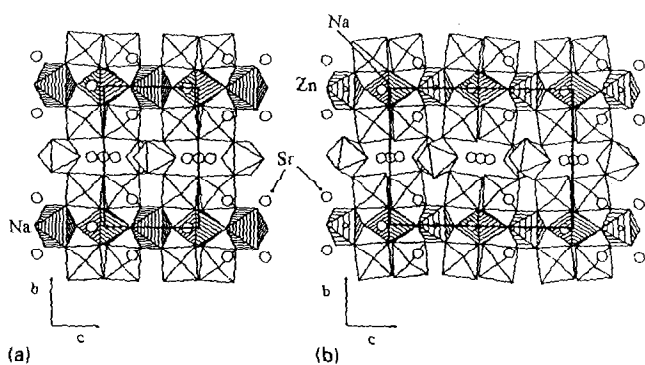


Fig. 1. (a) (100) projection of the $\text{Na}_2\text{Sr}_7\text{Al}_6\text{F}_{34}$ structure. View of an $[\text{Na}_2\text{Al}_6\text{F}_{34}]^{14-}$ sheet ($0.15 < x < 0.85$) and $[\text{Na}_2\text{F}_{10}]^{8-}$ chains. (b) (100) projection of $\text{Na}_2\text{Sr}_6\text{ZnFe}_6\text{F}_{34}$. View of an $[\text{NaZnFe}_6\text{F}_{34}]^{13-}$ sheet and $[\text{NaZnF}_{10}]^{7-}$ chains.

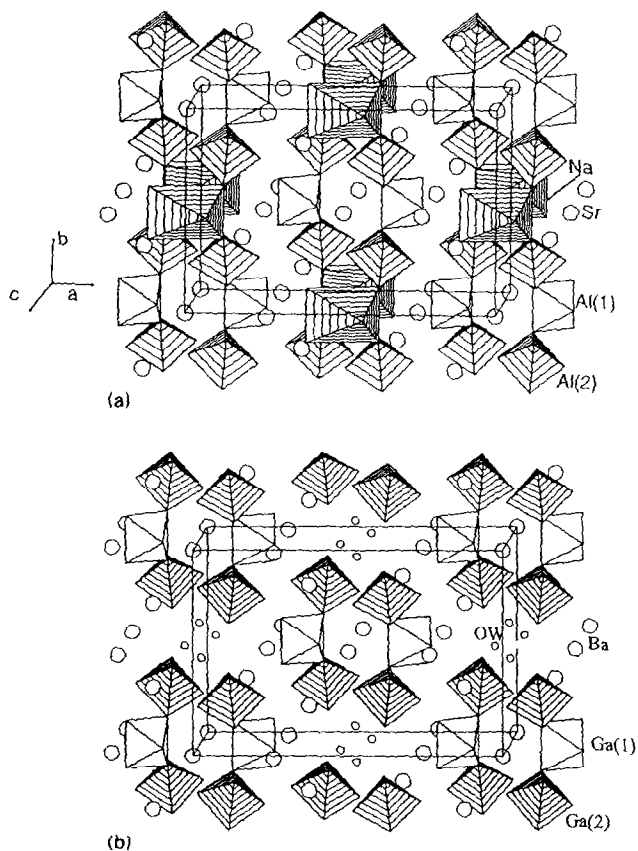


Fig. 2. (a) Perspective view of $\text{Na}_2\text{Sr}_7\text{Al}_6\text{F}_{34}$. (b) Perspective view of $\text{Ba}_7\text{Ga}_6(\text{F},\text{OH})_{32} \cdot 2\text{H}_2\text{O}$.

behaviour of the $\text{Ba}_7\text{M}^{\text{II}}\text{Fe}_6\text{F}_{34}$ ($\text{M}^{\text{II}} = \text{Mn}, \text{Fe}, \text{Cu}$) compounds. In contrast, in $\text{Na}_2\text{Sr}_7\text{Al}_6\text{F}_{34}$ the 2b and 2d sites are filled only by sodium cations ($r_{\text{Na}^+} = 1.02 \text{ \AA}$, $\text{CN} = 6$), whereas in the mineral and in $\text{Na}_2\text{Sr}_6\text{ZnFe}_6\text{F}_{34}$ the 2b site remains filled by a sodium ion but the 2d sites are occupied by a smaller cation ($r_{\text{Mg}^{2+}} = 0.72 \text{ \AA}$, $r_{\text{Zn}^{2+}} = 0.74 \text{ \AA}$, $\text{CN} = 6$). Thus, in $\text{Na}_2\text{Sr}_7\text{Al}_6\text{F}_{34}$, the mean distance $\text{Na}(1) - \text{F} = 2.23 \text{ \AA}$ of

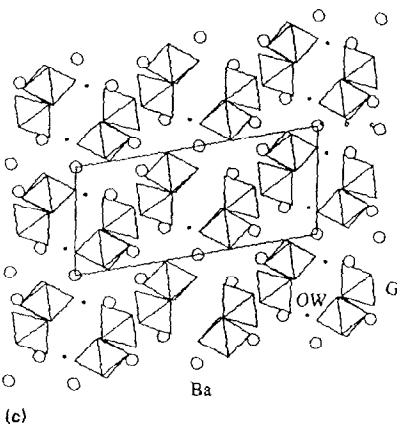
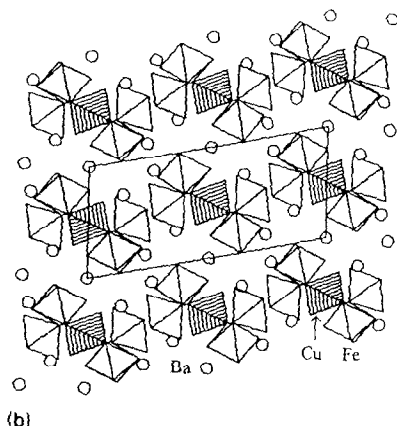
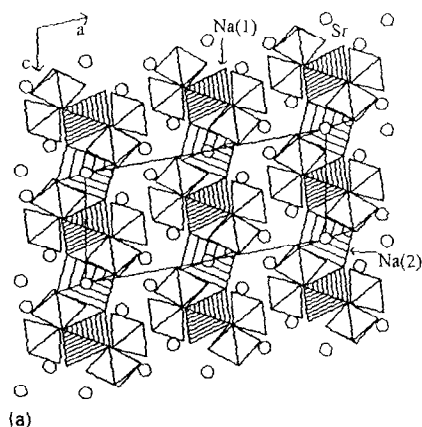


Fig. 3. Comparison of (010) projection of (a) $\text{Na}_2\text{Sr}_7\text{Al}_6\text{F}_{34}$, (b) $\text{Ba}_7\text{CuFe}_6\text{F}_{34}$ and (c) $\text{Ba}_7\text{Ga}_6(\text{F},\text{OH})_{32} \cdot 2\text{H}_2\text{O}$.

the 2d site is shorter than the sum of the ionic radii [19] (2.33 \AA).

Conclusions

Our structural studies show that fully ordered Jarlite, i.e. $\text{Na}_2\text{Sr}_7\text{Al}_6\text{F}_{34}$, can be obtained when the large divalent cationic sites (2a, 4i and 8j) are only filled by strontium. In contrast, a sodium-strontium disorder arises when at least one sodium cation is replaced by

a smaller one such as Zn^{2+} as in $(\text{NaZn})(\text{NaSr}_6)\text{Fe}_6\text{F}_{34}$. Hence, the Jarlite-type compounds $\text{M}^{\text{II}}_2(\text{Na}_2\text{Sr}_5)\text{Fe}_6\text{F}_{34}$, with two-dimensional magnetic behaviour, would be expected if two strontium ions were substituted by two divalent 3d cations. Solid-state syntheses are in progress to investigate this possibility. On the contrary, our studies show the existence of a 'very deficient' Jarlite, i.e. $\text{Ba}_7\text{Ga}_6(\text{F},\text{OH})_{32}\cdot 2\text{H}_2\text{O}$, when monovalent or smaller divalent cations ($r < 1.0 \text{ \AA}$) are absent. The isotypic iron compound has been synthesized and a Mössbauer study of the $[\text{Fe}_3(\text{F},\text{OH})_{16}]$ clusters undertaken.

Acknowledgments

The authors are indebted to Professor M. Leblanc and Dr R. Retoux for help in the X-ray data collection, and to H. Duroy who kindly performed the fluorine analysis by pyrohydrolysis.

References

- 1 A. Hemon, A. Le Bail and G. Courbion, *Eur. J. Solid State Inorg. Chem.*, **27** (1990) 905.
- 2 A. Hemon, A. Le Bail and G. Courbion, *J. Solid State Chem.*, **81** (1989) 299.
- 3 A. Hemon and G. Courbion, *Eur. J. Solid State Inorg. Chem.*, **29** (1992) 519.
- 4 A. Hemon and G. Courbion, *J. Solid State Chem.*, **81** (1989) 293.
- 5 F.C. Hawthorne, *Can. Mineral.*, **21** (1983) 553.
- 6 R. Bogvad, *Medd. Gronl.*, **92** (1933) 8.
- 7 C. Brosset, *Ph.D. Thesis*, University of Stockholm, Sweden, 1942.
- 8 R.B. Ferguson, *Am. Mineral.*, **34** (1949) 383.
- 9 J. Renaudin, G. Ferey, A. De Kozak and M. Samouel, *Rev. Chim. Miner.*, **27** (1987) 295.
- 10 A. Le Lirzin, J. Darriet, A. Tressaud and P. Hagenmuller, *C. R. Acad. Sci. Paris*, **308 II** (1989) 713.
- 11 J. Renaudin, G. Ferey, M. Drillon, A. De Kozak and M. Samouel, *C. R. Acad. Sci. Paris*, **308 II** (1989) 1217.
- 12 F. Plet, J.L. Fourquet, G. Courbion, M. Leblanc and R. De Pape, *J. Cryst. Growth*, **47** (1979) 699.
- 13 G. Courbion, *Thesis*, Le Mans, 1979.
- 14 J. Nouet, C. Jacoboni, G. Ferey, J.Y. Gerard and R. De Pape, *J. Cryst. Growth*, **8** (1970) 94.
- 15 W. Clegg, *Acta Crystallogr.*, **A37** (1981) 22.
- 16 G.M. Sheldrick, *SHELX76: Program for Crystal Structure Determination*, University of Cambridge, England, 1976.
- 17 *International Tables for X-ray Crystallography*, Kynoch Press, Birmingham, UK, 1968, Vol. IV.
- 18 G.M. Sheldrick, in G.M. Sheldrick, C. Kruger and R. Goddard (eds.), *Crystallographic Computing III*, Oxford University Press, Oxford, 1985, p. 175.
- 19 R.D. Shannon, *Acta Crystallogr.*, **A32** (1976) 75.
- 20 M.P. Crosnier and J.L. Fourquet, *Eur. J. Solid State Inorg. Chem.*, **29** (1992) 199.
- 21 M.P. Crosnier and J.L. Fourquet, *J. Solid State Chem.*, **99** (1992) 355.
- 22 N.E. Brese and M. O'Keeffe, *Acta Crystallogr.*, **B45** (1991) 192.
- 23 A. Hemon and G. Courbion, *J. Solid State Chem.*, **84** (1990) 115.
- 24 E. Herdtweck, J. Graulich and D. Babel, *Z. Naturforsch.*, **45b** (1990) 161.
- 25 D. Babel and A. Tressaud, in P. Hagenmuller (ed.), *Inorganic Fluorides*, Academic Press, New York, 1985, p. 77.
- 26 G. Courbion and G. Ferey, *J. Solid State Chem.*, **76** (1988) 426.
- 27 A. Hemon and G. Courbion, *J. Solid State Chem.*, **86** (1990) 246.
- 28 A. Hemon and G. Courbion, *J. Solid State Chem.*, **87** (1990) 344.
- 29 J. Renaudin, G. Ferey, A. De Kozak and M. Samouel, *Eur. J. Solid State Inorg. Chem.*, **27** (1990) 571.
- 30 J. Renaudin, G. Ferey, A. De Kozak and M. Samouel, *Eur. J. Solid State Inorg. Chem.*, **28** (1991) 373.
- 31 V.I. Simonov and B.V. Bukvetsky, *Acta Crystallogr.*, **B34** (1978) 355.